Eur. Phys. J. B **12**, 471–477 (1999)

THE EUROPEAN PHYSICAL JOURNAL B

EDP Sciences

Local triboelectricity on oxide surfaces

M. Saint Jean[a], S. Hudlet, C. Guthmann, and J. Berger

Groupe de Physique des Solides, Universités de Paris 6 et 7[b], Tour 23, 2 place Jussieu, 75251 Paris Cedex 05, France

Received 18 March 1998 and Received in final form 8 July 1998

Abstract. In triboelectric phenomena, electric charges are transferred when two materials are touched or rubbed together. We present in this paper a study of this effect performed on metallic oxides at the nanometric scale by an Atomic Force Microscope in the resonant mode. We show that following the electrification processes, positive or negative charges can be deposited. From our experimental data, we conclude that the charge transfer results in an equilibrium final state, the occupied states in the gap being "surface states" with large density and spread under the surface along a characteristic distance of about 100 nm.

PACS. 73.20.-r Surface and interface electron states – 73.40.-c Electronic transport in interface structures – 73.90.+f Other topics in electronic structure and electrical properties of surfaces, interfaces, and thin films

Introduction

Two neutral materials touched or rubbed together exchange electric charges. When these materials are separated, some of the charges are retained by each material which then appears as charged. This phenomenon is known as "the triboelectric effect". In spite of its long history and its industrial importance [1,2], this electrification phenomenon is poorly understood and various theoretical models have been proposed to analyse it. To test these models, we have studied triboelectricity on a nanometric scale carrying out experiments by the contact of a metallic oxide with the metallized tip of an Atomic Force Microscope.

Two kinds of theoretical models have been developed. Some of them assume that the insulator and the metal are in equilibrium after contact, the charge transfer is then such as to bring their electrochemical potentials into coincidence, the insulator electronic levels being bulk [3] or surface states [4]. In alternative models, the charge transfer corresponds to a mechanism where the final state is out of equilibrium [5]. Though different from each other, all these models predict a specific relationship between the transferred charge density σ_s and the initial electrochemical potential difference (hereafter denoted V_c and named "contact potential" by extension from the metal/metal contact case). To select one of these different models by investigating the relation $\sigma_s(V_c)$, numerous experiments have previously been done on the macroscopic scale [2]. Unfortunately, none of these experiments allows one to simultaneously measure the three relevant parameters involved in these models such as the transferred charge Q, the real exchange surface S, and the potential difference V_c. In the best case, only two of them were determined while some doubt remained about the last one.

To overcome these difficulties, we have used an Atomic Force Microscope in the resonant mode (AFMR) and exploited the opportunities offered by this new instrument. At first, the nanometric tip allows measurements over distances smaller than the roughness length (about 1 μm) which permits a well defined exchange surface whereas in previous experiments this surface has been widely discussed since there are important differences between the apparent and real exchange surfaces at the macroscopic scale. Further the use of modulation techniques in the resonant mode allows one to obtain simultaneously, measurements of the deposited charge, the contact potential V_c, and the surface topography. Several electrification experiments on polymeric surfaces [6] and silicon oxide [7] have been done recently on the nanometric scale. However, their purposes were quite different and concerned the studies of the stability of charge deposited by corona discharge; only one qualitative paper indicates the contact electrification of a polymeric surface [8].

In Section 1, we describe the experimental methods, in particular the charge depositing protocols, and the model that we have developed to analyse the data. The experimental results are presented in Section 2 and quantitatively discussed in Section 3.

[a] e-mail: saintjean@gps.jussieu.fr
[b] CNRS UMR 7588

1 Experimental methods and force modelization

1.1 Experimental set-up

The set-up of our experiments is very similar to the one previously described in reference [9], the main innovation is the addition of a vacuum chamber containing the sample and the tip, the interferometric detection remaining outside.

In these experiments, the nanometric metallic tip is fixed at the end of a cantilever which is excited at a frequency $\omega_{\rm m}$ selected near its resonance frequency ($\approx$ 200 kHz). When the tip interacts with an insulating surface fixed or grown on an underlying metallic electrode, the frequency and quality factor of the cantilever resonance are modified which induce a variation in the cantilever vibration amplitude $A(\omega_{\rm m})$ measured at $\omega_{\rm m}$. Moreover, if a modulated bias voltage $V = V_0 + V_1 \sin \Omega t$ ($V_1 = 5$ V, $\Omega \approx 20$ kHz) is applied to the tip, the underlying metallic surface being maintained at zero potential, an additional capacitive force $F(\Omega)$ is exerted on the tip and induces a cantilever oscillation $A(\Omega)$ at the frequency Ω. The cantilever vibration is measured by an optical heterodyne interferometric detection and analysed by two synchronous detectors respectively tuned at $\omega_{\rm m}$ and Ω frequencies. From the measurement of the amplitude $A(\Omega)$ we can determine the contact potential associated with the tip-surface system [9,10] and the deposited charge [8]. Without deposited charge, $A(\Omega)$ is proportional to $(V_0 + V_{\rm c})$; $V_{\rm c}$ is measured by varying V_0 until $A(\Omega)$ becomes zero which corresponds to $V_0 = -V_{\rm c}$. When a charge is on the surface, the additionnal charge-tip force induces a variation $A(\Omega)$ as the tip scans over the charge. By comparing $A(\Omega)$ before and after contact, the deposited charge can be determined (hereafter named "reading procedure"). Simultaneously, the output signal $A(\omega_{\rm m})$ is introduced into a feed-back loop to control the tip-surface distance. Moreover, the feed-back signal can be used to image the surface topography; in particular its corrugations can be explored before and after deposition.

Our experiments are performed on thin amorphous alumina films (thickness $D = 110$ nm) grown on aluminium. The samples are prepared by anodic oxidation in ammonium pentaborate ($NH_4B_5O_8$, $2H_2O$), a constant current, about 1 mA/cm^2, being imposed between the Al surface and the Pt cathode. By measuring the variation of the potential inside the oxide one can determine precisely its width. These oxides have been chosen for two reasons. First the mode of preparation results in very smooth surfaces without roughness. Moreover, previous studies have shown that the charges trapped on these oxides are very stable [7].

These samples are then transferred into the vacuum chamber of our experimental set up which is first outgassed over 24 hours before being filled with dry nitrogen gas to ensure that the oxide surface remains dry. Notice that no particular precautions are employed to avoid or reduce surface contamination. Indeed, we are much more interested by the mechanism of charge transfer itself than by the particular system studied. So, our purpose is to determine the specific relationship between the transferred charge density $\sigma_{\rm s}$ and the initial electrochemical potential difference whatever the origin of the electronic states occupied by the deposited charges and independently of the absolute values of the charge transfer.

For our experiments, we have chosen Si tips coated with Pt for both investigating the surface as well as depositing the charges on the oxides. From this last point of view, the Pt coating, corresponding to the metallic part in the metal/oxide contact, presents the advantage of being very stable and of maintaining a constant and uniform work function for a long time.

Two procedures of charge deposition have been followed. To clarify the possible deposition mechanisms, "injection experiments" have been first performed. In this type of experiment, the tip stays in contact with the same point of the oxide surface, a voltage $V_{\rm d}$ being applied to the tip. Initially far from the oxide, the tip is softly put in contact with the surface by slowly varying the reference value in the feedback loop. During this down motion, the tip is maintained at $V_0 = 0$. When the contact is established, a voltage $V_{\rm d}$ (-20 V $< V_{\rm d} < +20$ V) is applied for a time $t_{\rm d}$ (1 ms $< t_{\rm d} <$ 10 s) seconds, then the tip is raised far from the surface, the voltage $V_{\rm d}$, being, in this phase maintained for $t_{\rm r}$ seconds (1 ms $< t_{\rm r} <$ 10 s) to avoid any charge back flow [11]. After this up motion, the reading voltage V_0 is restored.

In the second type of experiment (hereafter called "friction experiments") the charge is transferred to the aluminium oxide by friction, the AFM tip and the underlying electrode being maintained at zero potential. In these experiments, the tip is slowly brought down to the oxide surface following a similar procedure to the "injection experiments" and scanned during 10 s along $L_0 = 500$ nm, the sweep frequency being 3 Hz.

We emphasise that in these procedures, the same tip is used for the deposition of charges and for reading. This requires very strict control on the conditions of the experiments. In particular we have verified, performing SEM studies on the tip before and after friction, that the tip and its "metallic coating" were not damaged during the experiments.

1.2 Force model

In these experiments, the acquired electrostatic data are the force amplitude $F(\Omega)$ at each point of the surface. Their analysis is complex and requires an adapted model, the electrostatic forces being long range interactions. Thus, we have developed a simple model describing the tip-surface force to determine the charge characteristics from the force maximum $F_{\rm max}$ and the width extension of the force measurements when the tip scans over the surface.

In this model, the tip is taken to be a sphere (radius R) the center of which is located at the distance $(R+z)$ from the surface and maintained at the potential $V_0 + V_1 \sin \Omega t$,

the width of the oxide layer being denoted by D. Following the procedure proposed in [12], R is determined by fitting the experimental variations of the force with the tip-surface distance. Using the results obtained previously [13] we obtain $R = 20$ nm. The deposited charges Q on the oxide are supposed extended over the surface on a spot characterized by its lateral extension L (note that the lateral extension L is not necessarily identical to the real contact extension L_0 since diffusion induced by the electric field during the deposition can spread the deposited charges, we shall return to this point in Sect. 3). The charge density (supposed uniform) is σ_s.

Following the procedure proposed by Terris *et al.* [8], we use the method of images to determine the electrostatic force between this effective tip and the surface. We have developed in a recent paper [14] a complete model of tip-surface electrostatic interaction. As a first order derivation is sufficient to determine $Q(V_d)$ or $\sigma_s(V_d)$, we neglect in this presentation the dielectric constant of the oxide (its effect could nevertheless be discussed by introducing an effective tip-surface distance). Since in our experiments z and $R \ll D$, our calculations show that the main contribution to the measured force $F(\Omega)$ modulated at Ω is due to the interaction between Q and $q_1 = 4\pi\varepsilon_0 R\,(V_0 + V_1 \sin \Omega t)$ which describes the tip charge due to the applied potential, all the other contributions being neglected.

In this frame, when $(R+z) > L$, the deposited charge distribution can be considered as a point charge Q; on the contrary, when the deposited charge extension is large or when the tip is very close to the oxide surface, $(R+z) < L$, then the deposited charges appear as an "infinite" uniform charged plane. In the first case, the AFMR data measure the deposited charge whereas in the second one, the charge density is measured. The $F(\Omega)$ amplitude maximum $F_{max}(\Omega)$ measured when the tip is just over the deposited charges can be evaluated in these two cases. The deposited charge distribution is then characterized by:

$$\text{for } (R+z) > L \qquad Q = \frac{\Delta F_{max}(\Omega)(R+z)^2}{V_1 R},$$

$$\text{for } (R+z) < L \qquad \sigma_s = \frac{\Delta F_{max}(\Omega)}{4\pi V_1 R}\,. \tag{1}$$

$\Delta F_{max}(\Omega)$ is the difference between the amplitude force $F_{max}(\Omega)$ measured just over the deposited charge and the amplitude $F_{min}(\Omega)$ measured far from this charge. The variations of the force when the tip scans the surface over the charge Q can also be calculated and the effects of the long range of the electrostatic forces appear very clearly. For the usually employed z value ($z, R \ll D$), the apparent force profile is roughly Gaussian like. Using the superposition principle, the calculation of the apparent dimension (defined as the Full Width Half Maximum) of a point charge measured by the tip is $R + z$. Generalized to a charge extended over L, this apparent charge size ΔL can be given by:

$$\Delta L = \alpha(z + R) + L \tag{2}$$

where α is a constant close to 1.

Note that when z is larger, the contribution of the deposited charge image $-Q$ in the underlying electrode has to be considered. This effect introduces dips on the edges of the "Gaussian" profile (Fig. 4) but the apparent charge size ΔL stays roughly given by $\alpha(z + R) + L$.

2 Variations of charge transfer with the contact potential

The aim of this work is to select between the different models describing the triboelectric effect for metal/metallic oxide systems. Whereas in classical experiments performed on a macroscopic scale the electrochemical potential difference is modified by substitution of the contacting metal, this potential difference is varied, in our experiments, by a change of the applied voltage V_d. Since the value of $\Delta F_{max}(\Omega)$ is proportional to the transferred charge Q or the surface charge density σ_s (relation (1)), we are able to determine easily the relations $Q(V_c)$ or $\sigma_s(V_c)$ from our "injection" experiments by measuring ΔF_{max} *versus* V_d.

2.1 Results

We have systematically studied the influence of the external parameters V_d, t_d and t_r on the charge transfer. No variation of the magnitude of the deposited charge was observed when the times t_d and t_r were varied between 1 ms and 10 s.

To test the influence of the applied potential V_d, we have deposited charges on the alumina surface along a straight line by doing 20 successive contacts, each one corresponding to a different applied voltage V_d which was varied by 2 V steps between ± 20 V. For each contact, the deposition time t_d and the removal time t_r were respectively 500 ms and 100 ms. After deposition, the force between the surface and the tip is measured with $V_0 = \pm 5$ V and $V_1 = 1$ V. In Figures 1a, b we present top view images of the electrostatic force amplitude detected after "injection" respectively with $V_0 = +5$ V and -5 V. The whole lateral extension of these images is 10 μm. We underline that these images are very stable and can be observed during many hours (in contrast, this stability is not observed for thinner samples; for $D = 10$ nm, the characteristic time of decrease of charge signal is only a few minutes). This indicates that the charges do not spread over the surface after the deposition and that we can neglect the surface conductivity of the oxide [15] at least for times higher than 1 ms which corresponds to the minimum time required between the deposition and the first measurement. On these electrostatic images we can observe a black-white line, the contrast of this line being inverted when the reading applied voltage is changed from 5 V to -5 V. Notice that in the same time the background is unchanged. This result is qualitatively in agreement with our model: for one tip polarity the Q-tip interaction is attractive whereas it is repulsive in the other polarity; in contrast the background

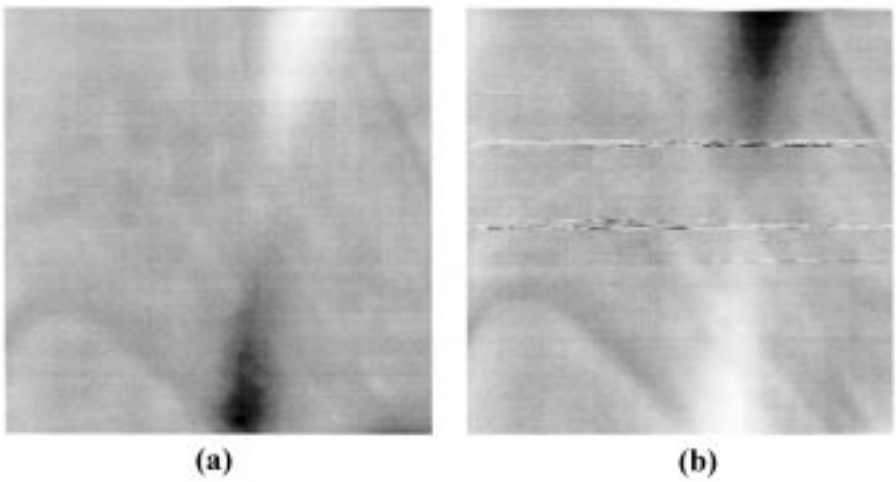

Fig. 1. Charges transferred during "Injection" experiments. The charges are deposited over a Al_2O_3 surface along a straight line by doing 20 successive contacts, each contact corresponding to a different applied voltage V_d which is varied between ± 20 V by 2 V steps. The complete image is 10 μm $\times$ 10 μm. (a) Electrostatic forces detected with $V_0 = 5$ V; (b) electrostatic forces detected with $V_0 = -5$ V.

due to the interaction between the tip and the underlying electrode is always capacitive and thus attractive whatever the tip polarity.

These images indicate without ambiguity that the charge transfer depends on the applied voltage. The deposited charge is roughly an odd function of the applied potential V_d, the black part of the image (1a) corresponds to a positive charge, whereas the white corresponds to a negative charge. Moreover, this transfer is reversible since the charge deposited with a potential V_d can be removed by applying at the same point the tip maintained at the inverse polarity $-V_d$. Finally, no surface deformation is observed on the topographic image.

The apparent deposition dimensions ΔL are larger than the tip surface distance z and the tip radius R (see Sect. 4). Thus, as discussed previously, the charge deposition has to be described by a surfacic charge density σ_s. Then the curve $\Delta F_{max}(V_d)$, obtained by plotting the force maximum ΔF_{max} *versus* the tip contact position, each point corresponding to a particular applied voltage V_d, is similar to the relation $\sigma_s(V_d)$. This plot is presented in Figure 2 where the left and right indices respectively correspond to the force ΔF_{max} and to the charge density σ_s values. On this curve, we can see that the charge density varies roughly linearly with the applied voltage without saturation for high applied potential. We observe that this plot appears as roughly continuous whereas the deposition is in fact a succession of spots. This behaviour is probably due to the diffusion of charges, assisted by the applied electric field, during the injection process. We shall return to this point in Section 3.

These results provide significant new information about the triboelectric effect and allow us to discuss the validity of the various proposed models. First, the charge transfer is achieved for $t_d = 1$ ms and does not increase for larger deposition times. Our experimental set-up does not allow exploration of smaller deposition times, nevertheless, whatever the real time of charge transfer is, the deposition time t_d is very short compared to the stability time observed (a few hours). Thus this charge transfer is rapid compared to the relaxation or diffusion processes and we can conclude that it results in an equilibrium final state.

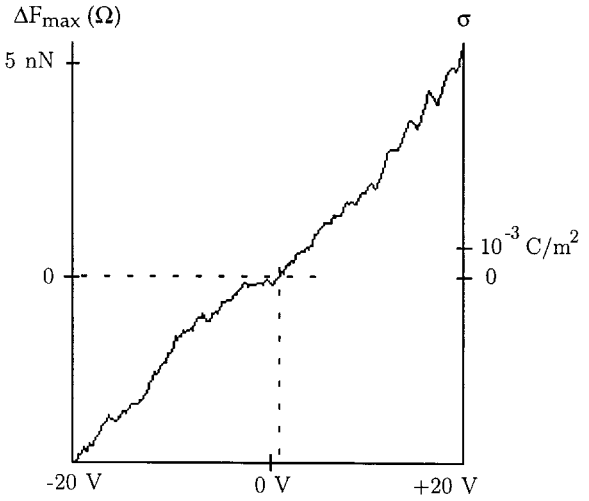

Fig. 2. Variations of the electrostatic force $\Delta F_{max}(\Omega)$ (left axis) and corresponding charge density σ_s (right axis) with the deposition potential V_d. The charges are deposited on an Al_2O_3 surface along a straight line, $\Delta F_{max}(V_d)$ is determined by drawing the force maximum $\Delta F_{max}(\Omega)$ *versus* the position on this line, each position corresponding to a specific deposition voltage. The charge density varies linearly with the applied voltage which corresponds to an equilibrium process between the tip and the "surface" states of the oxide surface.

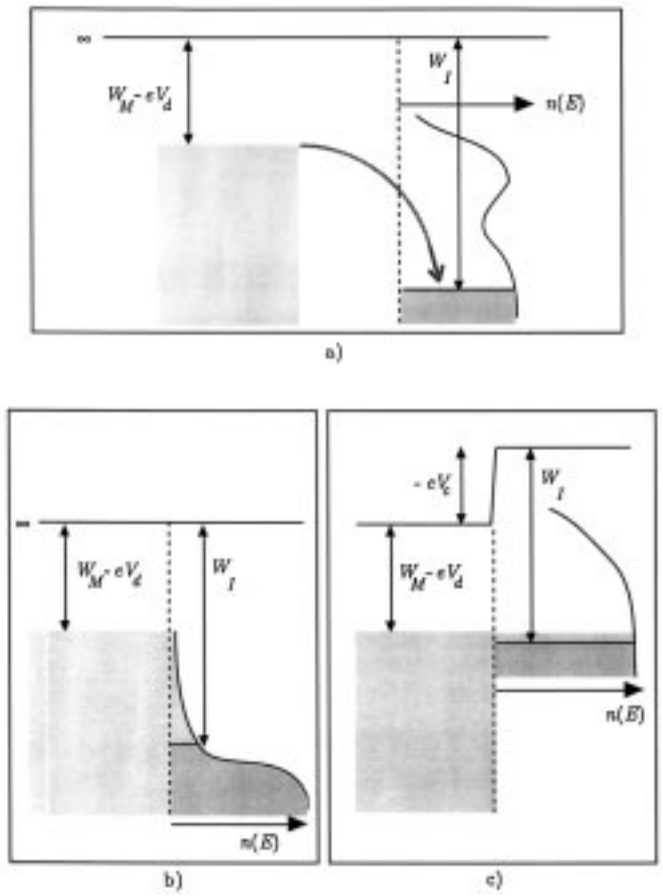

Fig. 3. Charge transfer mechanism on the "surface" states. $n(E)$ indicates the density of states of the insulator and W_I the energy of the first empty level before contact: (a) before contact; (b) for small density of states; (c) for large density of states.

The "equilibrium models" introduce oxide "bulk" and/or "surface" states to describe the electronic levels occupied by the deposited charges. In models using "bulk states", the charge density has to vary as $\exp\sqrt{V_\mathrm{c}}$ [3]; we have never observed this dependence in our experiments. In contrast, the linear variation of the transferred charge with the contact potential is in agreement with the models involving acceptor and donor levels in the gap on or just under the surface (named hereafter "surface trapped states") [2,4]. Thus we conclude that, in our experiments, the final state is an equilibrium between the metal and the oxide "surface states", these states being isolated from the bulk as it is suggested by the long stability time of the transferred charge. The general theory of this kind of mechanism has recently been described in a simplified form [16]. To discuss our results it is sufficient here to recognize that in this theory the surface state density $n(E)$ per unit energy is spread into the gap and to consider successively the two limiting cases, corresponding to small or large surface state density $n(E)$. As in every equilibrium model, the charge transfer occurs until the coincidence of the electrochemical levels of the two contacting systems. Thus, in our experiments, we have to compare before contact the energy of the first unoccupied level of the insulator denoted W_I to $(W_\mathrm{M} - eV_\mathrm{d})$, which is the work function of the metal tip W_M plus the applied energy $-eV_\mathrm{d}$ (Fig. 3a).

In the case of a small surface state density (Fig. 3b), only a few charges are transferred and no energy displacement of the levels has to be considered. To a first approximation, the transferred charge density is then given by:

$$\sigma_\mathrm{s} = -e \int_{W_\mathrm{I}}^{W_\mathrm{M}-eV_\mathrm{d}} n(E)\mathrm{d}E.$$

If we suppose that $n(E)$ is roughly constant and equal to n_0, the charge density obtained in this assumption is $\sigma_\mathrm{s} = n_0 e^2\ (V_\mathrm{c} + V_\mathrm{d})$ which is proportional to the applied voltage as found experimentally. Unfortunately this model results in a saturation for large applied potential since the charge transfer reaches a maximum as soon as $(W_\mathrm{M} - eV_\mathrm{d})$ occurs in the valence or conduction bands.

Alternatively, if we suppose that the surface state density is very important, the charge transfer induces a strong electrostatic potential which modifies the surface state energies; the coincidence of the electrochemical potentials is then reached even if a small range of energy in the gap is explored (Fig. 3c). In the ultimate case of a very large density $n(W_\mathrm{I})$ of the level W_I, the charges only transfer to this W_I level. This case corresponds to a linear variation of the charge density without saturation for high applied voltages, in agreement with our results. This high density of states cannot be explained by "surface states" strictly on the surface but could be understood if we suppose that the charges can jump, assisted by the applied electric field, to the levels just "under the surface" over a characteristic depth, a, and over a distance, L, on the surface. The long time stability of the deposition suggests that this characteristic "tunnelling" conduction distance is less large than the thickness of the alumina film D, the Al electrode does not act in this case as a charge collector; in contrast the rapid charge decrease observed for thinner samples suggests that a is larger than 50 nm. The same conclusion has been proposed for Si oxide to interpret the charge transfer obtained at the macroscopic scale [16].

3 Evaluation of charge transfer

The charge transfer mechanism seeming understood in these metallic oxides, we have now to compare the charge transfer in "friction" and "injection" experiments. Several authors suggest that different charge transfer mechanisms have to be involved to describe these kinds of experiments whereas others claim that the mechanisms are identical [2].

Figure 4 shows a typical electrostatic force image measured after a "friction experiment", the lateral extension being 1 μm $\times$ 1 μm. As for "injection experiments" these charges are very stable and can be still read without deformation after 24 h. Notice that on this image, we can observe the previously discussed dips associated

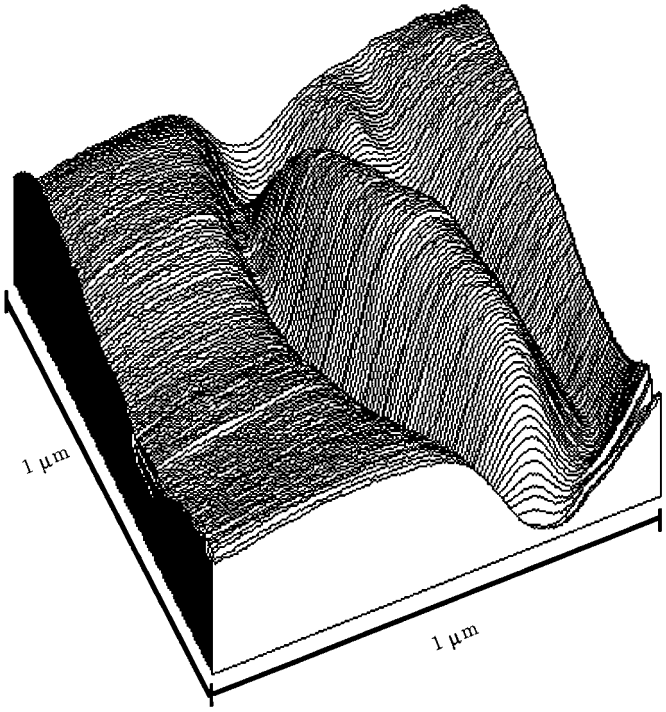

Fig. 4. Charges transferred during a "Friction" experiment. The charge is deposited with the Pt coated tip brought on the Al_2O_3 surface over a distance $L_0 = 500$ nm, the voltage between the tip and the underlying electrode being maintained to zero. Electrostatic force profile is measured with $V_0 = 5$ V. The deposited charges are electrons, $\sigma_s \approx -10^{-3}$ C/m^2.

with the influence of the Q image. These structures disappear when the tip-surface distance is reduced as for the images registered in injection experiments.

The image analysis indicates that the deposited charge is negative. As indicated in Section 2, the real contact surface during the deposition is roughly $(L_0 \times 2R)$ corresponding to (500 nm × 40 nm). By measuring the force distribution, the charge distribution appears spread over a much larger characteristic distance $(\Delta L \times \Delta l)$, of about (770 nm × 300 nm). These apparent dimensions can not be explained by the long range of the electrostatic force since, from relation 2 this long range force effect (with $R = 20$ nm and $z = 30$ nm) would result in apparent dimensions $[L_0 + \alpha(R + z)] \times [2R + \alpha(R + z)]$ about (550 nm × 90 nm), smaller than those which are measured. Then to explain these large dimensions, we have to consider a possible diffusion of the deposited charges on/and in the oxide surface during the deposition; this diffusion being probably assisted by the strong electric field (higher than 10^7 V/m) existing between the tip and the surface. This diffusion can be characterized by an isotropic length X. Then, the real deposition surface would be in fact $S_d = (L_0 + 2X) \times (2R + 2X)$ instead of $(L_0 \times 2R)$ and the apparent dimensions of the deposition would be $(\Delta L \times \Delta l)$ where $\Delta L = [\alpha(z+R)+L_0+2X]$ and $\Delta l = [\alpha(z + R) + 2R + 2X]$. In this frame, the diffusion length X can be evaluated from the experimental data to about 100 nm. Using these values and those of the force maximum $\Delta F_{max}(\Omega) = 3 \times 10^{-9}$ N, the charge density σ_s can be evaluated to about 2.3×10^{-3} C/m^2. The total exchanged charge is then $Q = \sigma_s S_d$ is 4×10^{-16} C which corresponds to 2 500 electrons.

The "injection experiments can be analysed in the same frame. Using the data presented in Figure 1, the charge density varies between 0 and 20×10^{-3} C/m^2, the slope σ_s/V_d being about 10^{-3} C/Vm^2. The transferred charge is zero when the applied voltage $V_d = 1$ V, which means that in this case the contact potential V_c is completely compensated by the applied voltage, $V_c = -1$ V. When $V_d = 0$, the charge density is about -10^{-3} C/m^2. The sign and the intensity of these charges are both coherent with the corresponding results in "friction" experiments. Moreover, these results are in agreement with those previously obtained in macroscopic experiments performed on a Au/SiO_2 contact or Mg/SiO_2 contact which also exhibit linear variation of the charge with the applied voltage [16,17]. In these last experiments, the deposited charge increases as 5×10^{-12} C/V between −10 and 10 V whereas the charge density per volt corresponding to these experiments is 2×10^{-3} C/Vm^2 [18].

In these two electrification experiments, it is really surprising that the deposited charges induce near the surface an electric field with a value (10^8–10^9 V/m) which is much higher than the breakdown electric field, which is about 3×10^6 V/m. Nevertheless, this observation has also been made on a macroscopic scale by other authors who indicate an electric field of about 10^8 V/m without breakdown [2]. This effect can be explained by the fact that the tip surface distance is smaller than the ionic free path which is about 1 μm in ambient atmosphere [19].

4 Conclusion

We have studied the charge transfer between a metallized tip and a metallic oxide surface during contact or friction experiments. Following the electrification processes, positive or negative charges can be deposited and erased. Our experimental data show that the charge transfer results in an equilibrium final state. The transferred charge and its density vary linearly with the "contact" potential between the insulator and the metal. No saturation effect is observed in the range of -20 V $< V_c <$ 20 V. We conclude that the occupied states in the gap are states with large density. These states are spread on the surface over a characteristic distance of about 100 nm and in the oxide over a depth larger than 50 nm. These "surface states" are certainly isolated from the purely bulk states, since the charge density varies linearly with V_d (in the case of a complete equilibrium between the tip and the oxide, the variation would be exponential). It would be very interesting to determine the nature of these states. Some authors suggest, as an attempt to understand their macroscopic data, that these states originate from the surface deformation [2,4]. Our results, however, seem to weaken this assumption. Our topographic pictures, indeed, do not exhibit any plastic surface deformation though the local

pressure applied on the sample is equal to 10^9 Pa (100 nN applied to a surface of about 100 nm^2), which is closer to the Young's modulus of the oxide ($E = 10^{11}$ Pa) than the pressure exerted in classical macroscopic experiments (10^4 Pa). Moreover, the transferred charge density is of the same order in friction and contact experiments; this suggests that these states are intrinsic and do not depend on the electrification process. These levels could be those theoretically described in metal/oxide contacts [20].

References

1. J.A. Cross, *Electrostatics: Principles, Problems and Applications* (Bristol, Hilger, 1987).
2. J. Lowell, A.C. Rose-Innes, Adv. Phys. **29**, 947 (1980).
3. A.M. Cowley, S.M. Sze, J. Appl. Phys. **36**, 3212 (1965).
4. D.A. Hays, D.K. Donald, *Annual Rep. Conf. Electrical Insulation and Dielectric Phenomena* (Washington, National Academy of Science, 1972).
5. D.E. Ioannou, Physica B **90**, 277 (1977).
6. C. Schonenberger, Phys. Rev. B **45**, 3861 (1992) and references therein.
7. S. Morita, Y. Sugawara, Y. Fukano, Jpn. J. Appl. Phys. **32**, 2983 (1993) and references therein.
8. B.D. Terris, J.E. Stern, D. Rugar, H.J. Mamin, Phys. Rev. Lett. **63**, 2669 (1989).
9. Y. Martin, C.C. Williams, H.K. Wickramasinghe, J. Appl. Phys. **61**, 4723 (1987).
10. M. Saint Jean, S. Hudlet, C. Guthmann, J. Berger, Phys. Rev. B **56**, 1 (1997).
11. A. Wahlin, G. Backstrom, J. Appl. Phys. **45**, 2058 (1974).
12. H.W. Hao, A. Baro, J. Saenz, J. Vac. Sci. Technol. B **9**, 1323 (1991).
13. S. Hudlet, M. Saint Jean, C. Guthmann, J. Berger, Eur. Phys. J. B **2**, 5 (1998).
14. M. Saint Jean, S. Hudlet, C. Guthmann, J. Berger, to appear in J. Appl. Phys. (1999).
15. T. Tsuyuguchi, T. Uchihashi, T. Okusako, Y. Sugawara, S. Morita, Y. Yamanishi, T. Oasa, Jpn. J. Appl. Phys. **33**, L1046 (1994).
16. A. Labads, J. Lowell, J. Phys. D: Appl. Phys. **24**, 1461 (1991).
17. A.R. Akande, J. Lowell, J. Phys. D: Appl. Phys. **20**, 565 (1987).
18. J. Lowell, J. Phys. D: Appl. Phys. **23**, 1082 (1990).
19. W. Harper, *Contact and Frictinal electrification* (Oxford University Press, 1967).
20. C. Noguera, G. Bordier, J. Phys. III France **4**, 1851 (1994).